

## Spin separation in digital ferromagnetic heterostructures

J. Fernández-Rossier\* and L. J. Sham

*Department of Physics, University of California San Diego, 9500 Gilman Drive, La Jolla, California 92093*

(Received 18 January 2002; revised manuscript received 16 April 2002; published 30 August 2002)

In a study of the ferromagnetic phase of a multilayer digital ferromagnetic semiconductor in the mean-field and effective-mass approximations, we find the exchange interaction to have the dominant energy scale of the problem, effectively controlling the spatial distribution of the carrier spins in the digital ferromagnetic heterostructures. In the ferromagnetic phase, the majority-spin and minority-spin carriers tend to be in different regions of the space (spin separation). Hence, the charge distribution of carriers also changes noticeably from the ferromagnetic to the paramagnetic phase. An example of a design to exploit these phenomena is given here.

DOI: 10.1103/PhysRevB.66.073312

PACS number(s): 75.70.Cn, 75.50.Pp, 75.10.-b

The research in proactive use of the spins of the carriers to add a new dimension to electronics starts a new area known as spintronics.<sup>1</sup> The recent discoveries<sup>2,3</sup> of ferromagnetism with high Curie temperatures in a number of conventional semiconductors doped with magnetic impurities hold promise for the implementation of spintronics in semiconductors.

Inhomogeneously doped semiconductors, such as the  $p$ - $n$  junction, play a crucial role in conventional electronic devices. Their properties depend on the distribution of the itinerant carriers, which is governed by the Coulomb interaction of the carriers with the impurities and with other carriers. In this paper we study the charge and spin distributions of the itinerant carriers in semiconductors  $\delta$  doped with magnetic impurities, such as GaMnAs.<sup>4,5</sup> Our theory is within the mean-field, effective-mass, and virtual-crystal approximations. In addition to the electrostatic forces, the itinerant carriers have an exchange interaction with the magnetic impurities. Our calculation shows that the magnetization of the high Mn concentration in the  $\delta$  layers in the ferromagnetic phase gives rise to a spin-dependent potential experienced by the carriers comparable in order of magnitude to the charge potential of the  $\delta$  layer. The effect of the spin-dependent potential on the inhomogeneous spin distribution of the carriers was noted by Loureiro da Silva *et al.*<sup>6</sup> in multilayered GaMnAs with 5% magnetic impurities. By contrast, the  $\delta$  doping with a nominal concentration per atomic plane of 25–50% Mn atoms gives rise to a qualitatively different phenomenon of spin separation. This creates the possibility of the magnetic control of the itinerant carriers by manipulating the magnetization of the Mn ions. In particular, the spin-dependent potential may be used to influence the spin dependence of the distribution of itinerant carriers. The majority carriers<sup>7</sup> accumulate in the region of the Mn layers whereas minority carriers are repelled from the Mn region. In the paramagnetic phase, the spin potential averages to zero and the magnetic influence disappears. To show the potential of the spin separation for device applications, we give an example of how heterostructures may be designed to engender spin separation.

This paper is organized as follows. A brief review of the relevant theoretical formalism precedes the application to establish the general principle of magnetic control and to show how it works in two specific systems. The first is the experi-

mental system of multiple digital layers of Refs. 4 and 5. We find the phenomenon of spin separation in the ferromagnetic phase. Specifically, for appropriate carrier densities and interlayer distances, the minority carriers are located mainly in the interlayer spacer, with a very small overlap with the magnetic atoms whereas the majority carriers are mainly located in the layers of magnetic atoms. Second, we design a double GaAs quantum well with AlGaAs barriers and a  $\delta$  layer of Mn in the middle of one well and a  $\delta$  layer of an acceptor (Be) in the middle of the other. When the GaMnAs well is changed from the paramagnetic phase to the ferromagnetic phase, a net transfer of charge and spin from the Be well to the Mn well is produced, because of the appearance of the dominant magnetic interaction. As a result, there is a potential drop across the structure as well as a spin polarization in the Be well.

Our calculations are based on the mean-field model,<sup>8–12,6</sup> with two types of spins: localized  $d$  electrons with magnetic moments of  $5/2$  Bohr magnetons and itinerant carriers (holes because of the Mn and Be doping). There is a Heisenberg spin exchange between the itinerant carrier and the Mn  $d$  electron, which is responsible for the ferromagnetism. The hole energy bands are based on the effective-mass approximation with the kinetic energy given by the bands of the host GaAs. The effective potential induced by the dopants is the only change for the carrier subbands, as in the virtual crystal approximation. The Coulomb interaction between the holes is taken into account in the Hartree approximation. The in-plane energy dispersion of the holes subbands is described by a parabolic model that neglects the spin-orbit interaction. The omission of the spin-orbit effect, which has also been used in Refs. 6 and 8–10, greatly simplifies the numerical computation. On the other hand, it leads to an overestimate of the polarization of the Mn spins induced by the interaction with the carriers. We correct for this by using a smaller value of the coupling constant  $J$  of the Heisenberg exchange, which reproduces the Curie temperature obtained in our previous calculation including the spin-orbit interaction.<sup>12</sup> Because the charge and spin distributions are averaged properties of the system, we argue that the qualitative aspects of the effects discussed in this paper would remain if the spin-orbit interaction is included.

Both model systems studied here are taken to be translationally invariant in the  $x$ - $y$  plane normal to the growth axis.

Thus, the Mn concentration  $c_M(z)$  varies only along the  $z$  axis. We assume that, in addition to the magnetic impurities that act as acceptors in GaMnAs, there is a distribution of donors,  $c_c(z)$ , which partially compensates the Mn acceptors, so that the total density of holes is smaller than the density of Mn, as is observed.<sup>2</sup> For simplicity, we assume that the spatial distributions of the donor and acceptor impurities are the same except for a multiplicative constant. From the charge neutrality condition,  $P + C_c = C_M$ , where  $P$ ,  $C_c$ , and  $C_M$  are the average densities of holes, of the compensating impurities, and of the Mn impurities, respectively.

In the mean-field approximation, the effect of the magnetic impurities on the itinerant carriers is given by a spin-dependent potential:

$$V_\sigma = \frac{J\sigma}{2} c_M(z) \langle M(z) \rangle, \quad (1)$$

where  $\sigma = \pm 1$  denotes the spin directions,  $J$  is the exchange-coupling constant between the itinerant carrier and the Mn spin, and  $\langle M(z) \rangle$  stands for the local average magnetization of Mn. The Mn polarization is produced by the molecular field created by the spin polarization of the itinerant carriers as well as the external magnetic field. At temperature  $T$  and zero external magnetic field, the Mn magnetization is given by the usual Brillouin function:

$$M(z) = SB_S \left( \frac{J}{k_B T} \frac{p_+(z) - p_-(z)}{2} \right), \quad (2)$$

where  $p_\sigma(z)$  is the spin-dependent density of the itinerant carriers.

The effective Schrödinger equation for the holes has a self-consistent potential  $V_e(z) + V_\sigma(z)$ , where  $V_e(z)$  is the electrostatic potential experienced by the hole and is given by,

$$\frac{d^2}{dz^2} V_e(z) = \frac{4\pi e^2}{\epsilon} [c_c(z) - c_M(z) + p_+(z) + p_-(z)]. \quad (3)$$

The hole eigenenergy is the sum of the quantized energy  $E_{n,\sigma}$  from the motion in the  $z$  direction and the plane-wave energy  $\epsilon_{\vec{k}_\parallel} = \hbar^2 k_\parallel^2 / 2m_\parallel$  from the in-plane motion. The hole wave function is the product of the bound-state envelope function in  $z$  times the plane wave normal to the  $z$  axis. The spin-dependent hole density is given by:

$$p_\sigma(z) = \sum_n \int \frac{d^2 \vec{k}_\parallel}{(2\pi)^2} \frac{|\phi_{n,\sigma}(z)|^2}{e^{(E_{n,\sigma} + \epsilon_{\vec{k}_\parallel} - \mu)/k_B T} + 1}, \quad (4)$$

where  $\mu$  is the chemical potential.

It is illuminating to estimate the strength of the spin-dependent potential (1) for a single magnetic digital layer. Throughout the paper we take the hole effective-mass tensor to be  $m_\parallel = 0.11$  and  $m_z = 0.37$  times the free-electron mass and model the distribution of the Mn in a digital layer as Gaussian:

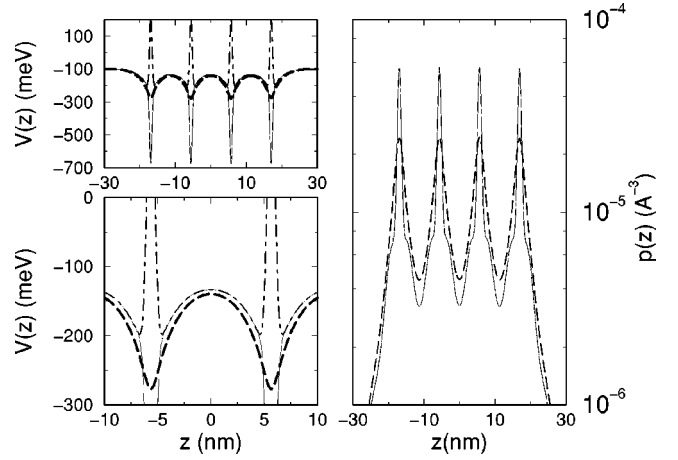


FIG. 1. Left upper panel: spin-dependent potentials for majority carriers (solid line) and minority (thin dot-dashed line) at  $T=5$  K (the ferromagnetic phase) and total potential at  $T=40$  K (the paramagnetic phase) (thick dashed line). Left bottom panel: magnification of the upper panel. Right panel: total carrier density profiles for  $T=5$  K (solid line, the ferromagnetic case) for  $T=40$  K (long-dashed line, the paramagnetic case). Notice the logarithmic scale in the vertical axis.

$$c_M(z) = \frac{C_M}{\sqrt{\pi}\Delta} \exp[-(z/\Delta)^2]. \quad (5)$$

In a digital layer of  $\text{Ga}_{0.5}\text{Mn}_{0.5}\text{As}$  the total concentration of Mn is  $C_M = 3.13 \times 10^{14} \text{ cm}^{-2} = 3.13 \text{ nm}^{-2}$ . Transmission electron microscopy experiments<sup>4</sup> reveal that the Mn is spread over two or three atomic planes. This corresponds roughly to the Gaussian half-width of  $\Delta = 0.5 \text{ nm}$ . The exchange integral of  $J = 150 \text{ meV nm}^3$  used in our previous work<sup>12</sup> to calculate the Curie temperature is reduced to  $J = 100 \text{ meV nm}^3$  here in order to compensate the absence of spin orbit in the present calculation. The maximum of the spin-dependent potential in Eq. (1) for saturated magnetization is 441.5 meV in comparison with the charge well depth of about 177 meV. The peak to valley splitting is twice the maximum value. In a diluted magnetic semiconductor quantum well, the magnetic potential is one order of magnitude smaller than in a digital layer. Hence, the magnetic control is more practical in digital layers than in quantum wells.

The magnetic potential is attractive for the majority carriers and repulsive for the minority carriers. As the temperature is increased, the magnetization decreases and so does the magnetic potential, vanishing above the Curie temperature. Accordingly, the itinerant carrier density profiles change significantly as the temperature varies. Both the potentials and the density profiles are shown in Fig. 1 for a system of  $N = 4$  digital layers, with an interlayer separation  $D = 40 \text{ ML}$  (GaAs monolayers), or 11.3 nm, and a density of holes per layer  $p = 1.3 \times 10^{13} \text{ cm}^{-2}$ . In order to improve numerical convergence, we locate 100 meV step potential barriers at  $z = \pm 50 \text{ nm}$ . Similar results are obtained for systems between 1 and 10 layers. In the left panels of Fig. 1 we present the potential profiles at  $T=40$  K (thick dashed line), when the system is paramagnetic. In the same panels we show the

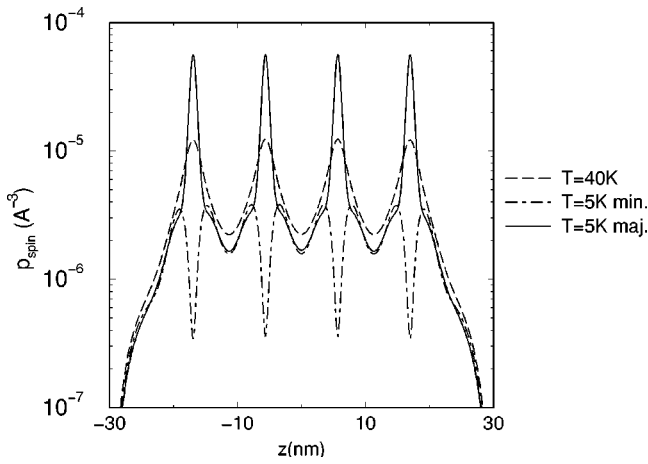


FIG. 2. Spin-dependent hole density profiles for  $T=5$  K majority carriers (solid), minority carriers (long dashed), and for  $T=40$  K (long dashed).

total potential for majority (attractive) and minority (repulsive) carriers for spin-dependent potentials at  $T=5$  K when the system is ferromagnetic. The lower panel is a magnification of the center of the upper panel. There it can be better appreciated the potential in the paramagnetic phase, whose only contribution is electrostatic. The large magnitude of the spin-dependent part of the potential is apparent in the upper left panel. The effect on the density profile of the itinerant carriers is shown in the right panel. In the ferromagnetic case (thin solid line) the carriers tend to pile up in the magnetic layers. In the paramagnetic case (long-dashed line) the carrier distribution is more spread out, with more carriers in the spacer layers relative to the ferromagnetic case.

Figure 2 shows the resultant spin-dependent density profiles for two temperatures. In the ferromagnetic case, the distributions of majority and minority carriers are distinct. The majority carriers are localized in the magnetic layers whereas the minority carriers are almost totally expelled from it (notice the logarithmic scale in the vertical axis). This “spin separation” phenomenon is, of course, absent in the paramagnetic case. We have checked that as the interlayer distance decreases or the hole density increases the spin separation diminishes. Spin fluctuations of Mn beyond the mean-field approximation are a major source of spin-flip scattering. Hence, we expect the spin-flip scattering to be reduced when the spin separation is larger.

Results of Fig. 1 show how the exchange interaction can overcome the electrostatic interactions in the case of a digital layer. We propose here a heterostructure in which this effect is made more apparent and can be measured. It is a double quantum well of GaAs with GaAsAl barriers,  $\delta$  doped with one layer of Mn in the middle of the left well and one layer of the acceptor Be in the middle of the right well. For illustration but not necessity, we choose the density profile of the Be to be identical to that of the Mn ions plus its compensating charges. We take the density of holes per digital layer in either well of  $1.3 \times 10^{13} \text{ cm}^{-2}$ . The digital layer of Mn has a total density of  $3.13 \times 10^{13} \text{ cm}^{-2}$  and a Gaussian distribution as in Eq. (5) with  $\Delta=0.5$  nm.

Above the Curie temperature the system is totally symmetric (by the construction of the model) and so is the charge

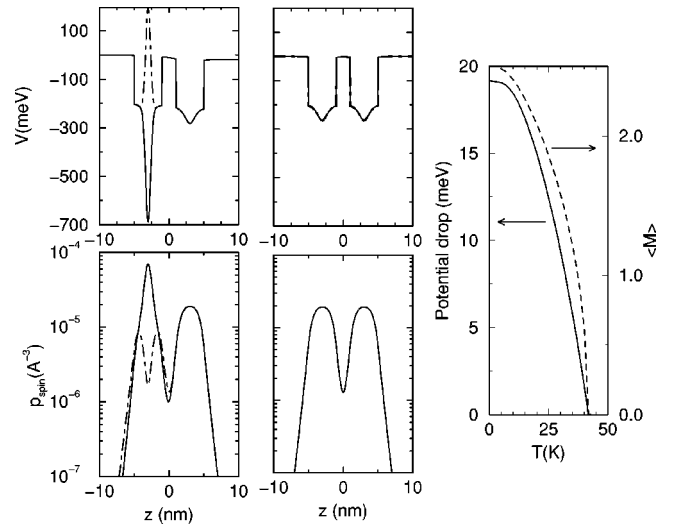


FIG. 3. Left upper/lower panels: spin-dependent potentials/density profiles for majority holes (solid line) and minority holes (thin dot-dashed line) at  $T=5$  K (the ferromagnetic phase). The middle panels: spin-dependent potentials and density distributions at  $T=40$  K (the paramagnetic phase)—same notation as above. Right panel: potential drop (solid line) and magnetization (dashed line) versus temperature.

distribution (shown in the middle column of Fig. 3). At low temperatures the majority carriers with spin antiparallel to the Mn are attracted by the magnetic layer. As a result, there is a spin-dependent charge transfer from the nonmagnetic to the magnetic well (the left column of Fig. 3), which generates an internal electric field and a potential drop. In the rightmost panel we plot both the potential drop and the Mn average magnetization as a function of the temperature. The potential drops follow the average magnetization and their maximum is close to 20 meV at zero temperature. Larger values can be obtained for smaller carrier densities, but this decreases the Curie temperature.<sup>12</sup> The charge imbalance is  $1.2 \times 10^{12} \text{ cm}^{-2}$  or 4.6% of the total hole density. The charge-transfer effect also takes place for other values of the carrier density, as well as for structures with a different density of Be and Mn. As a result of the rearrangement of the carriers in the heterostructure, as the system goes from the paramagnetic to the ferromagnetic phase, large changes in the in-plane and vertical transport properties can be expected as well.

Tight-binding calculations for a superlattice of digital GaAs/GaAsMn (Ref. 13) give very similar results to those obtained using an envelope function approach,<sup>12</sup> validating the use of the effective-mass approximation in  $\delta$  doped systems. A density functional-calculation for a superlattice of digital GaAs/MnAs predicts a half-metallic behavior.<sup>14</sup> Our results should be compared with a similar calculation including compensating impurities, 50% of Mn and larger interlayer distances.

In conclusion, we have studied the spatial distribution of the carrier spins in digital ferromagnetic heterostructures. Our main results are: (i) The distribution of carriers in digital ferromagnetic heterostructures of GaAsMn is largely controlled by the exchange interaction that overcomes the electrostatic interaction. (ii) Large changes in the spatial distri-

bution of carriers take place when ferromagnetism is switched off (for instance, by increasing the temperature above the Curie temperature). (iii) In some situations the minority carriers are totally separated from the Mn layers and the majority carriers. This might have consequences in transport properties and the anomalous Hall effect.

We wish to thank D. D. Awschalom, R. Kawakami, A. Gossard, E. Gwinn, L. Brey, and B. H. Lee for stimulating discussions. We acknowledge the Spanish Ministry of Education for financial support and support by Grant Nos. DARPA/ONR N0014-99-1-109 and NSF DMR 0099572.

---

\*Present Address: Department of Physics, University of Texas at Austin, Austin, TX 78712.

<sup>1</sup>S.A. Wolf and D. Treger, *IEEE Trans. Magn.* **36**, 2748 (2000).

<sup>2</sup>H. Ohno *et al.*, *Appl. Phys. Lett.* **69**, 363 (1996); A. Van Esch *et al.*, *Phys. Rev. B* **56**, 13103 (1997).

<sup>3</sup>S. Sonoda *et al.*, cond-mat/0108159; M.L. Reed *et al.*, *Appl. Phys. Lett.* **79**, 3473 (2001).

<sup>4</sup>R.K. Kawakami *et al.*, *Appl. Phys. Lett.* **77**, 2379 (2000).

<sup>5</sup>X. Chen *et al.*, *Bull. Am. Phys. Soc.* **46**, 508 (2001); cond-mat/0203361 (unpublished); G. Kioseoglou *et al.*, *Appl. Phys. Lett.* **80**, 1150 (2002).

<sup>6</sup>L. Loureiro da Silva *et al.*, *Appl. Phys. Lett.* **79**, 3305 (2001).

<sup>7</sup>Throughout the paper the words majority and minority carriers refer to the spin degree of freedom. The word carrier refers always to the holes, which are the relevant particles in the system

of interest (III-V-Mn semiconductors).

<sup>8</sup>T. Jungwirth, W.A. Atkinson, B.H. Lee, and A.H. MacDonald, *Phys. Rev. B* **59**, 9818 (1999).

<sup>9</sup>B. Lee, T. Jungwirth, and A.H. MacDonald, *Phys. Rev. B* **61**, 15606 (2000); L. Brey and F. Guinea, *Phys. Rev. Lett.* **85**, 2384 (2000).

<sup>10</sup>A. Ghazali, I.C. da Cunha Lima, and M.A. Boselli, *Phys. Rev. B* **63**, 153305 (2001).

<sup>11</sup>T. Dietl *et al.*, *Science* **287**, 1019 (2000); T. Dietl, H. Ohno, and F. Matsukura, *Phys. Rev. B* **63**, 195205 (2001).

<sup>12</sup>J. Fernández-Rossier and L.J. Sham, *Phys. Rev. B* **64**, 235323 (2001).

<sup>13</sup>I. Vurgaftman and J.R. Meyer, *Phys. Rev. B* **64**, 245207 (2001).

<sup>14</sup>S. Sanvito and N.A. Hill, *Phys. Rev. Lett.* **87**, 267202 (2001).